Chapter 17
Stress Determination for Granular Materials Using TSA: An Inverse Approach

Mohammad Yousefi, Xavier Balandraud, and Wael A. Samad

Abstract Granular materials are among the materials which do not fall within the traditional definition of matter. The behavior of granular materials is of great importance in fields such as chemical and agronomical industries, since many of the materials used are prepared from powders or grains, or in geotechnical engineering due to discrete nature of soils. Extensive research has been done to study and quantify the contact force network on various granular systems, specifically the contact force distribution in terms of magnitudes and orientations. However, the stress magnitudes in the contact zones have always been a challenge, regardless of the full-field method used in the analysis. The objective of the work presented here is to determine the stresses in two-dimensional granular materials from a thermoelastic stress analysis (TSA) test using an inverse approach. The inverse approach relies on both the TSA values in the vicinity of the interparticle contacts, an extension of superposed Flamant solutions for concentrated forces on surfaces, as well as static equilibrium equations. Preliminary results on a periodic stacking of cylinders show promising perspectives for granular materials.

Keywords Infrared thermography · Granular material · TSA · Hybrid-TSA · Flamant solution · Inverse technique

Introduction

Granular materials are composed of grains with various sizes, shapes and constitutive materials. They are widely used in many industrial fields. Sands, soils and rocks are involved in civil engineering for instance. Cereals, sugar and rice are used in the agro-food processing industry. Pharmaceutical industry employs raw granular materials for preparing medical drugs. Discrete matters have mechanical behaviors differing from those of solids, liquids and gases [1]. Their global mechanical response is governed by the interparticle contact forces [2]. Different approaches by simulation have been employed to study the influence of various parameters: size and shape of the particles [3–5], friction properties [6], surface energy [7] and properties of the base materials [8] Different experimental approaches are also available, in particular full-field measurement techniques, to identify the contact force network of granular systems subjected to macroscopic mechanical loadings.

Non-contact full-field measurement techniques have also been employed for various types of material, but applications to granular media are relatively rare compared with continuous media. This can be explained by the three-dimensional nature of media such as sands, requiring measurements in the volume and thus limiting the number of techniques available such as X-ray tomography combined with volumetric digital image correlation [9, 10]. Two-dimensional (2D) granular systems have been also analyzed using suitable 2D full-field measurement techniques. Many applications concern cylinders placed in parallel, forming so-called Schneebeli materials [11]. Optical imaging was combined with digital image correlation (DIC) to perform the particle image velocimetry (PIV) technique and then measure the rigid-body displacements of the particles and the strains of the granular system [12–14]. DIC was also used to measure strains in the particles themselves [15–18]. Finally,

M. Yousefi · W. A. Samad (✉)
Rochester Institute of Technology, Dubai, UAE
e-mail: mmy3147@g.rit.edu; wascad@rit.edu

X. Balandraud
Université Clermont Auvergne, CNRS, SIGMA Clermont, Institut Pascal, Clermont-Ferrand, France
e-mail: xavier.balandraud@sigma-clermont.fr

A. Baldi et al. (eds.), *Residual Stress, Thermomechanics & Infrared Imaging and Inverse Problems, Volume 6*,
Conference Proceedings of the Society for Experimental Mechanics Series, https://doi.org/10.1007/978-3-030-30098-2_17

two full-field measurement techniques are available to measure stresses in the particles. Photoelasticimetry was employed to measure shear stresses in birefringent particles [19–21]. Infrared (IR) thermography was also carried out to measure fields of hydrostatic stress in granular systems by thermoelastic stress analysis (TSA) [8, 22, 23].

Extensive research has been done to study and quantify the contact force networks on granular systems, specifically the contact force distribution in terms of magnitudes and orientations. Photoelastic data and DIC data combined with Granular Element Method or Finite Element Method were used to identify these force networks [16–18, 24]. However, the stress magnitudes in the contact zones have always been a challenge, regardless of the full-field method used in the analysis. The objective of the present work is to identify stresses in a 2D granular material from TSA data and using an inverse approach. The latter relies on the TSA values in the vicinity of the interparticle contacts, an extension of superposed Flamant solutions for concentrated forces on surfaces, as well as static equilibrium equations. Previous work has shown the possibility of reconstructing stress contours on simpler loading scenarios (e.g. Brazilian test) [25], but has not been extended to more complicated periodic stacking scenarios.

It is worth mentioning that the analytical-Flamant and experimental-TSA coupling presented here was made possible thanks to the prior successes in hybridizing TSA measurements. Most of the research came out of the Experimental Mechanics Group at the University of Wisconsin—Madison where over the years, coupled isopachic stresses (in the form of $\sigma_x + \sigma_y$) were separated and reconstructed using a hybrid experimental-analytical formulations. Hybrid-TSA method was applied to various geometries and loading scenarios such as: circular holes [26], elliptical holes [27], irregularly shaped cutouts [28], pinned-connections and bolted structures [29] and diametrically loaded disks [30]. For more information on Hybrid-TSA, comprehensive review papers can be found in [31].

The paper is divided in three sections as follows. The first section presents the experimental test providing TSA data in a 2D periodic granular system under confined compression. The second section provides the background about Flamant solutions. The third section presents the results obtained.

Experimental Test

Figure 17.1 presents a schematic view of the experimental device used for the mechanical test under study. The granular system is composed of cylinders made in POM polymer with the same diameter (8 mm), forming thus a 2D quasi-periodic monodisperse organization. The frame and the top horizontal wall are made of steel and can be considered non-deformable compared to the granular material subjected to confined compression. The mechanical loading was performed using a ±15 kN MTS uniaxial testing machine. A force-controlled sinusoidal signal was applied at a frequency of 3 Hz. The maximum compression force was fixed to −5 kN for a load ratio of 0.1. A Cedip Jade III-MWIR camera was employed for temperature measurements. It features a wavelength range of 3.5–5 μm, a sensor size of 320 × 240 pixels and a Noise Equivalent Temperature Difference (NETD) of 0.02 °C. The granular system was preliminary painted in black to maximize the thermal emissivity of the observed surfaces. The acquisition frequency was set to 147 Hz.

Figure 17.2a presents the TSA data (in °C), namely the amplitudes of temperature oscillation at the frequency of the mechanical loading. Assuming an adiabatic response, these data can be considered as proportional to the hydrostatic stress. It can be noted that the observed surface are "free" by definition, meaning that they are in a plane stress state. As a consequence, the TSA data can be considered as proportional to the sum of the two principal stresses. Following comments can be done from

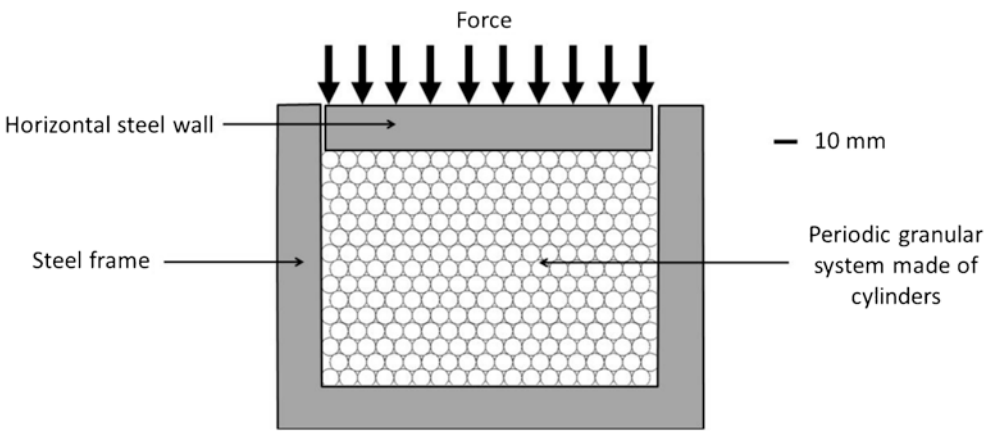

Fig. 17.1 Schematic view of the experimental system used for the mechanical test. An IR camera was employed to measure the temperature changes on the end of the cylinders during cyclic confined compression

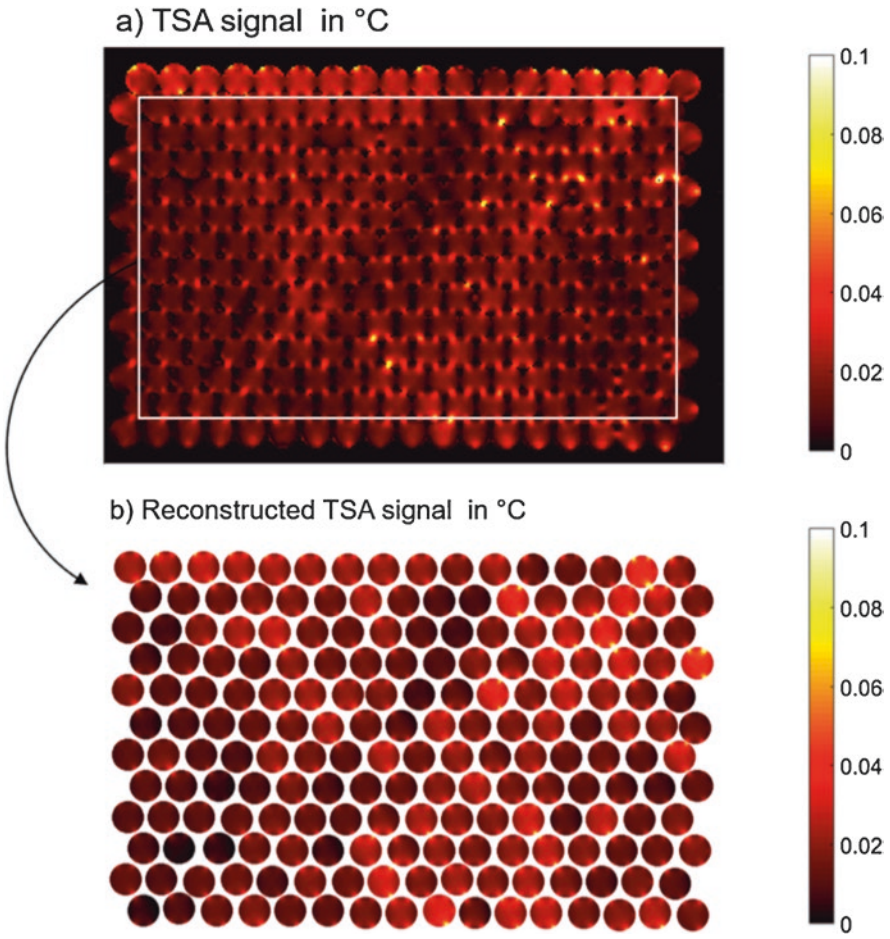

Fig. 17.2 (**a**) Data obtained by TSA approach, (**b**) reconstructed TSA image. Boundary cylinders have been removed in the reconstructed image

this figure. First, the field of TSA data is not periodic. This result is not surprising because the geometric periodicity cannot be achieved in an actual monodisperse granular material (actual ratio between frame's width and particle diameter different from the theoretical one). Moreover it is well known that the contact force network is impacted by slight local fluctuations in the base material and the particle shapes. In the present experiment, large triangular patterns can be visualized in Fig. 17.2a. Second, although each cylinder is in theory in contact with six surrounding particles (except at the contact with the frame and the top horizontal wall), only four contact generally transfer force. This result is typical of periodic monodisperse systems. Third, they are cylinders with three and five contacts transferring forces. Last, it can be noted that the weak spatial resolution of the field of TSA data prevents clear analysis. Flamant solutions can be advantageously employed to improve the raw data, as shown in Fig. 17.2b and explained in the next sections. Note that Fig. 17.2b shows small gaps between the different cylinders. This is due to the fact that the Flamant solution goes to infinity right at the contact location, and was as such avoided.

Background About Flamant Solutions

Flamant's problem aims to identify the stress fields caused by a force acting normal to the surface of a half plane. Apply thing to this analytical formulation to the case of a diametrically loaded disk is shown in Fig. 17.3.

Notice that this case involves the summation of two Flamant solutions, each in its own coordinate system, and then adding a radial tension component so that traction free boundary conditions on the outer surface of the disk is maintained.

The three individual components of stress for Flamant's problem are shown below, where F is the magnitude of the contact force and the Cartesian system origin is centered about the point of application of the force, F:

$$\sigma_x = \sigma_r \cos^2\theta = -\frac{2Fx^2y}{\pi\left(x^2+y^2\right)^2} \tag{17.1}$$

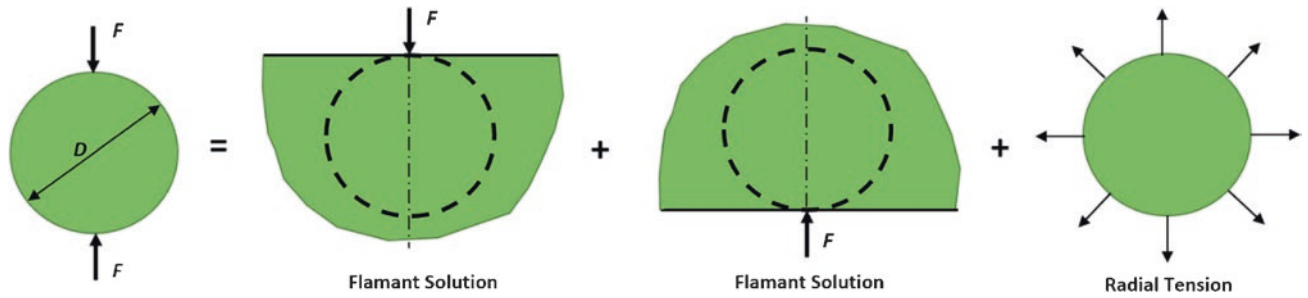

Fig. 17.3 Flamant's case: half-plane subjected to a normal force at the surface for the case of a diametrically loaded disk

$$\sigma_y = \sigma_r \sin^2\theta = -\frac{2Fy^3}{\pi\left(x^2+y^2\right)^2} \tag{17.2}$$

$$\tau_{xy} = \sigma_r \sin\theta\cos\theta = -\frac{2Fxy^2}{\pi\left(x^2+y^2\right)^2} \tag{17.3}$$

With the additional radial tension stress shown below:

$$\sigma_{radial} = \frac{2F}{\pi D} \tag{17.4}$$

For the case of a stacking of disks involving several contacts, the individual Flamant solutions for each contact location would have its own force magnitude; F in Eqs. (17.1)–(17.3). With this being an inverse approach, where the TSA full-field stresses are used to retrieve the contact forces, $F's$, the thermoelastic quantities $(\sigma_x + \sigma_y)$ are expressed in terms of the Flamant solution as shown in the equation below:

$$\sigma_x + \sigma_y = -\left[\left[\frac{2Fx^2y}{\pi\left(x^2+y^2\right)^2}\times\sin\left(\theta+\frac{\pi}{2}\right)\right]+\left[\frac{2Fx^2y}{\pi\left(x^2+y^2\right)^2}\times\cos\left(\theta+\frac{\pi}{2}\right)\right]+\left[\frac{2Fy^3}{\pi\left(x^2+y^2\right)^2}\times\cos\left(\theta\right)\right]+\left[\frac{2Fy^3}{\pi\left(x^2+y^2\right)^2}\times\sin\left(\theta\right)\right]\right] \tag{17.5}$$

Equation (17.5) can be then factored and written in the following simplified form below:

$$K_{i,k} = F_i \times \left[\frac{\left(-2x_k^2y_k\left(\sin\left(\theta_k+\frac{\pi}{2}\right)+\cos\left(\theta_k+\frac{\pi}{2}\right)\right)+\left(-2y_k^3\left(\cos\left(\theta_k\right)+\sin\left(\theta_k\right)\right)\right)\right)}{\pi\left(x_k^2+y_k^2\right)^2}\right] \tag{17.6}$$

where i is the increment representing the contact force number index, and k is the increment describing the location relative to the force application. Both i and k start from 1 and terminate at n, the total number of contact forces for a given disk, resulting in a square matrix, $K_{n\times x}$.

Note that for this generalized case, Eq. (17.4) of the radial component of stress does not exactly apply. As such, the resultant component of the radial stress is expressed in terms of the contact forces, F_1 through F_n, and set to zero as shown in the equation below so that the determined contact forces conform to the traction-free conditions.

$$R_n = \sigma_{rn} = F_n \times \left[-\frac{2x_n^2y_n}{\cos^2\left(\tan^{-1}\left(\frac{y_n}{x_n}\right)\right)\pi\left(x_n^2+y_n^2\right)^2}\right] = 0 \tag{17.7}$$

Moreover, and to add validity to the inversely determined contact forces, static equilibrium conditions are expressed again in terms of all the present contact forces.

$$\sum_1^n F_x = 0 \tag{17.8}$$

$$\sum_1^n F_y = 0 \tag{17.9}$$

with that Eqs. (17.6)–(17.9) are compiled together in the matrix equation below, where all the contact forces can be solved for using a linear-least squares approach:

$$\begin{bmatrix} K_{1,1} & \cdots & K_{1,n} \\ \vdots & K_{i,k} & \vdots \\ K_{1,n} & \cdots & K_{n,n} \\ -\cos(\theta_1) & \cdots & -\cos(\theta_n) \\ -\sin(\theta_1) & \cdots & -\sin(\theta_n) \\ R_1 & \cdots & R_n \end{bmatrix} \begin{bmatrix} F_1 \\ \vdots \\ F_n \end{bmatrix} = \begin{bmatrix} (\sigma_x + \sigma_y)_1 \\ \vdots \\ (\sigma_x + \sigma_y)_n \\ 0 \\ 0 \\ 0 \end{bmatrix} \tag{17.10}$$

Having determined the contact forces, those can now be substituted back in the analytical expressions of stresses from the superposed Flamant solutions discussed earlier.

Application to the 2D Periodic Granular System

Figure 17.4a shows a snapshot of Fig. 17.2 in the bottom right-hand side of the granular material. The processing is focused on seven cylinders, indicated with white circles in the image. The TSA data at the six contacts of each cylinder were extracted to reconstruct the TSA signal: see Fig. 17.4b. Additionally, TSA stresses are now separated and made available full-field in the x and y directions as shown in Fig. 17.4c, d respectively. This is of great importance as now high magnitude stress networks can be identified in the both directions.

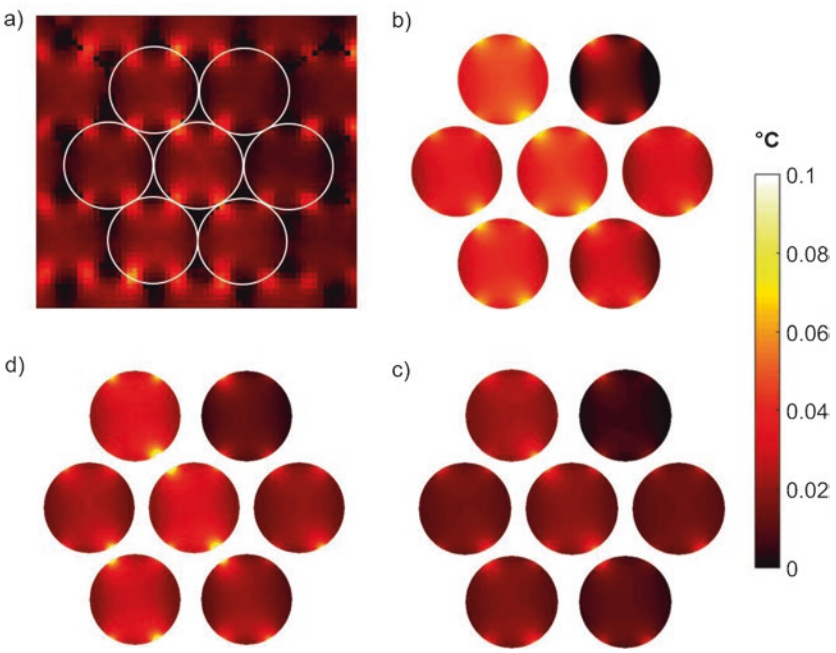

Fig. 17.4 Full-field stresses: (**a**) raw TSA data, and the reconstructed stress fields via Flamant solutions of (**b**) TSA, (**c**) σ_x and (**d**) σ_y

Conclusion

Granular materials exhibit contact force networks when they are submitted to macroscopic mechanical loading. Identification of such networks is of prime interest to understand the mechanical response of these materials. In the present study, a quasi-periodic granular media was built from cylinders placed in parallel and then submitted to cyclic confined compression. IR thermography was employed to extract data related to the thermoelastic coupling featured by the base material (TSA approach). Then an inverse approach based on an extension of superposed Flamant solutions for concentrated forces on surfaces, as well as static equilibrium equations, was performed to reconstruct the TSA signal. Preliminary results show promising perspective for various stacking scenarios of granular materials.

Acknowledgements The authors gratefully acknowledge Dr. Chanwit Chaiamarit, Dr. Pawarut Jongchansitto and Prof. Itthichai Preechawuttipong from Chiang Mai University, Thailand for the discussions about the mechanical response of granular materials. Ms. Rym Boufayed, Université Clermont-Auvergne, France is also acknowledged for the help in image processing.

References

1. H.M. Jaeger, S.R. Nagel, Granular solids, liquids, and gases. Rev. Mod. Phys. **68**, 1259–1272 (1996)
2. S. Ostojic, E. Somfai, B. Nienhuis, Scale invariance and universality of force networks in static granular matter. Nature **439**, 828–830 (2006)
3. D.H. Nguyen, E. Azéma, F. Radjai, P. Sornay, Effect of size polydispersity versus particle shape in dense granular media. Phys. Rev. E **90**, 012202 (2014)
4. A.A. Peña, R. García-Rojo, H.J. Herrmann, Influence of particle shape on sheared dense granular media. Granul. Matter **9**, 279–291 (2007)
5. C. Nouguier-Lehon, B. Cambou, E. Vincens, Influence of particle shape and angularity on the behaviour of granular materials: a numerical analysis. Int. J. Numer. Anal. Methods Geomech. **27**, 1207–1226 (2003)
6. S.G. Bardenhagen, J.U. Brackbill, D. Sulsky, Numerical study of stress distribution in sheared granular material in two dimensions. Phys. Rev. E **62**, 3882–3890 (2000)
7. I. Preechawuttipong, R. Peyroux, F. Radjai, W. Rangsri, Static states of cohesive granular media. J. Mech. Sci. Technol. **21**, 1957–1963 (2007)
8. P. Jongchansitto, I. Preechawuttipong, X. Balandraud, M. Grédiac, Numerical investigation of the influence of particle size and particle number ratios on texture and force transmission in binary granular composites. Powder Technol. **308**, 324–333 (2017)
9. H. Wolf, D. Konig, T. Triantafyllidis, Experimental investigation of shear band patterns in granular material. J. Struct. Geol. **25**, 1229–1240 (2003)
10. S.A. Hall, M. Bornert, J. Desrues, Y. Pannier, N. Lenoir, G. Viggiani, P. Besuelle, Discrete and continuum analysis of localised deformation in sand using X-ray μCT and volumetric digital image correlation. Geotechnique **60**, 315–322 (2010)
11. G. Schneebeli, Une analogie mécanique pour les terres sans cohésion. C. R. Hebd. Acad. Sci. **243**, 125–126 (1956)
12. C. Slominski, M. Niedostatkiewicz, J. Tejchman, Application of particle image velocimetry (PIV) for deformation measurement during granular silo flow. Powder Technol. **173**, 1–18 (2007)
13. S.A. Hall, D.M. Wood, E. Ibraim, G. Viggiani, Localised deformation patterning in 2D granular materials revealed by digital image correlation. Granul. Matter **12**, 1–14 (2010)
14. V. Richefeu, G. Combe, G. Viggiani, An experimental assessment of displacement fluctuations in a 2D granular material subjected to shear. Geotech. Lett. **2**, 113–118 (2012)
15. E. Marteau, J.E. Andrade, A novel experimental device for investigating the multiscale behavior of granular materials under shear. Granul. Matter **19**, 77 (2017)
16. R. Hurley, E. Marteau, G. Ravichandran, J.E. Andrade, Extracting inter-particle forces in opaque granular materials: beyond photoelasticity. J. Mech. Phys. Solids **63**, 154–166 (2014)
17. R.C. Hurley, K.W. Lim, G. Ravichandran, J.E. Andrade, Dynamic inter-particle force inference in granular materials: method and application. Exp. Mech. **56**, 217–229 (2016)
18. N. Karanjgaokar, Evaluation of energy contributions using inter-particle forces in granular materials under impact loading. Granul. Matter **19**, 36 (2017)
19. A. Shukla, C. Damania, Experimental investigation of wave velocity and dynamic contact stresses in an assembly of disks. Exp. Mech. **27**, 268–281 (1987)
20. K.M. Roessig, J.C. Foster, S.G. Bardenhagen, Dynamic stress chain formation in a two-dimensional particle bed. Exp. Mech. **42**, 329–337 (2002)
21. S.A. Mirbagheri, E. Ceniceros, M. Jabbarzadeh, et al., Sensitively photoelastic biocompatible gelatin spheres for investigation of locomotion in granular media. Exp. Mech. **55**, 427–438 (2015)
22. C. Chaiamarit, X. Balandraud, I. Preechawuttipong, M. Grédiac, Stress network analysis of 2D non-cohesive polydisperse granular materials using infrared thermography. Exp. Mech. **39**, 761–769 (2015)
23. P. Jongchansitto, X. Balandraud, M. Grédiac, C. Beitone, I. Preechawuttipong, Using infrared thermography to study hydrostatic stress networks in granular materials. Soft Matter **10**, 8603–8607 (2014)
24. T.S. Majmudar, R.P. Behringer, Contact force measurements and stress-induced anisotropy in granular materials. Nature **435**, 1079–1082 (2005)

25. M. Yousefi, X. Balandraud, W.A. Samad, Thermographic stress field investigation of a multiply-loaded disk, in *Residual Stress Thermomechanics & Infrared Imaging, Hybrid Techniques and Inverse Problems*, vol. 7 (Springer, Cham, 2019), pp. 115–117
26. S. Lin, D. Matthys, R.E. Rowlands, Separating stresses thermoelastically in a central circularly perforated plate using an airy stress function. Strain **45**, 516–526 (2009)
27. A.A. Khaja, R.E. Rowlands, Experimentally determined stresses associated with elliptical holes using polar coordinates. Strain **49**, 116–124 (2013)
28. W.A. Samad, R.E. Rowlands, Full-field thermoelastic stress analysis of a finite structure containing an irregularly-shaped hole. Exp. Mech. **54**, 457–469 (2014)
29. W.A. Samad, A.A. Khaja, A. Kaliyanda, R.E. Rowlands, Hybrid thermoelastic stress analysis of a pinned joint. Exp. Mech. **54**, 515–525 (2014)
30. B. Foust, R.E. Rowlands, Thermoelastic determination of individual stresses in a diametrally loaded disk. Strain **47**, 146–153 (2011)
31. S. Lin, W.A. Samad, A.A. Khaja, R.E. Rowlands, Hybrid thermoelastic stress analysis. Exp. Mech. **55**, 653–665 (2015)